Available online at www.sciencedirect.com
SCIENCE DIRECT®
Journal of Power Sources 142 (2005) 117–124
JOURNAL OF POWER SOURCES
www.elsevier.com/locate/jpowsour

Pressure drop behavior in the anode flow field of liquid feed direct methanol fuel cells

H. Yang, T.S. Zhao*, Q. Ye

Department of Mechanical Engineering, The Hong Kong University of Science and Technology, Clear Water Bay, Kowloon, Hong Kong SAR, China

Received 25 August 2004; accepted 15 September 2004
Available online 8 December 2004

Abstract

In this work, we experimentally investigated the two-phase flow pressure drop behavior in the anode flow field of an in-house fabricated direct methanol fuel cell (DMFC). The anode flow field consisted of a single serpentine flow channel with a cross-sectional area of $2.0 \times 2.0\,mm^2$ and a total length of 420 mm. The pressure drops between the inlet and the outlet of the flow channel were measured by varying current density. The experimental results show that at low current densities, the pressure drop increased with increasing current density. After reaching a peak at certain current density, however, the pressure drop began to decrease with increasing current density. It has also been shown that the pressure drop always increased with the methanol solution flow rate. However, either lower or higher flow rates deteriorated the cell performance. The experimental results further show that the pressure drop became almost independent of the current density when the methanol solution flow rate became sufficiently high. The study also reveals that both temperature and methanol concentration had significant influence on the cell performance, but their effects on the pressure drop were small.

Keywords: Direct methanol fuel cells; Serpentine channel; Two-phase flow; Pressure drop

1. Introduction

As compared with conventional hydrogen feed PEM fuel cells, a liquid feed direct methanol fuel cell (DMFC), using a solid polymer membrane as electrolyte and liquid methanol as fuel, offers some unique advantages, including lower system volume and weight, simpler system design, simpler mode of operation with fast response and better dynamics as well as lower investment and operating costs [1–5]. Thus, it has been projected as a promising power source for portable electronic devices, electric vehicles, and other mobile and stationery applications. Driven by these needs, there has been strong effort from university researchers and industry engineers all over the world to focus on the research and development of DMFCs. Most of the previous studies have been focused on the electrochemical aspects of DMFCs, such as the improvement of the electro-activity of methanol oxidation on anode by exploring more active electro-catalysts [6–9], the optimization cathode electrode structures to avoid severe flooding [10–12], and reduction of the substantial methanol crossover by modifying existing polymer membranes or searching for alternatives [13–20]. However, relatively few papers have been reported on the study of the flow dynamics aspect in the anode flow field. One of the problems in this aspect is the pressure drop behavior in the flow field, which is needed to size a proper pump for the auxiliary fuel supply system. Clearly, a reduction in the pumping power consumed for the fuel supply system increases the overall DMFC system efficiency. Therefore, the study of the pressure drop behavior in the anode flow field is essential for the design and optimization of a DMFC system.

In the DMFC, methanol solution is fed into the anode flow field and diffuses to the catalyst sites through the gas diffusion layer, while the reaction-produced gas CO_2 at the catalyst layer transport backward into the anode channels through the

* Corresponding author. Tel.: +852 2358 8647; fax: +852 2358 1543.
E-mail address: metzhao@ust.hk (T.S. Zhao).

0378-7753/$ – see front matter © 2004 Elsevier B.V. All rights reserved.
doi:10.1016/j.jpowsour.2004.09.036

gas diffusion layer. Therefore, a liquid–gas two-phase flow, consisting of methanol solution and reaction-produced gas CO_2, exists in the anode flow field under typical DMFC operating conditions. In general, the total pressure drop of a two-phase flow consists of frictional, acceleration and gravitational components [21,22]. The two-phase flow in the anode flow field of a DMFC is different from the conventional co-current liquid–gas two-phase flow in a channel with gas and liquid uniformly entering from one of its ends. In the DMFC, liquid methanol solution is fed to the inlet of the flow field, while gas CO_2 enters the flow channel from the diffusion layer. In such a special two-phase flow system, the increase in void fraction of gas CO_2 with channel length leads to not only an increase in the liquid velocity [23], but also an increase in the average specific volume of two-phase fluid along the flow channel. The increased two-phase flow velocity causes the frictional pressure drop to increase, while the increased average specific volume leads to an increase in the acceleration pressure drop. On the other hand, however, the increase in void fraction of gas CO_2 also decreases the average density of two-phase fluid in the flow field, causing the gravitational pressure drop to decrease. Clearly, the total pressure drop behavior is affected by void fraction of gas CO_2 in the flow channel, i.e. the amount of gas CO_2 generated during fuel cell operation, which is directly related to the cell current density.

It appears that the only studies related to the pressure drop behavior in the anode flow field of a DMFC are due to Argyropoulos et al. [24,25]. They developed a pressure drop model for a DMFC consisting of a parallel flow field based on the homogenous two-phase flow theory, with which, they analyzed the effects of various operation parameters on the pressure drop behavior.

In this paper, we report on in situ measurements of the pressure drop across the anode flow field of a DMFC consisting of a single serpentine flow channel. We show how the pressure drop varied when current density was increased. We have also investigated the effects of various operation parameters, including methanol solution flow rates, cell operating temperatures and methanol concentrations, on the pressure drops and cell performance.

2. Experimental

2.1. Transparent DMFC

A transparent DMFC was designed and fabricated for this study, as schematically shown in Fig. 1. The membrane electrode assembly (MEA), detailed in the subsequent paragraph, was sandwiched between two flow field plates with a PTFE gasket onto either side of the MEA. This assembly, including the flow field plates and the MEA, was clamped between the two enclosure plates by eight M8 screw joints, each having a torque of about 3 N m. As can also be seen from Fig. 1, in addition to two pieces of PTFE gasket, two rubber gaskets

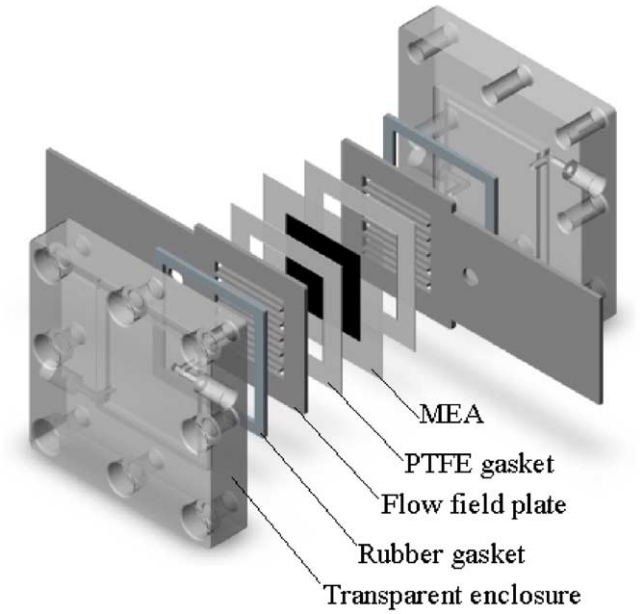

Fig. 1. In-house fabricated DMFC.

were employed between the flow field plates and enclosure plates to prevent leakage of fuel and oxidant.

The MEA, fabricated in this work, had an active area of $4.0 \times 4.0\,cm^2$ and consisted of two single-side ELAT electrodes from E-TEK and a Nafion® membrane 115. Both anode and cathode electrodes used carbon cloth (E-TEK, Type 'A') as the backing support layer with 30% PTFE wet-proofing treatment. The catalyst loading on the anode side was $4.0\,mg\,cm^{-2}$ with unsupported [Pt:Ru] Ox (1:1 a/o), while the catalyst loading on the cathode side was $2.0\,mg\,cm^{-2}$ using 40% Pt on Vulcan XC-72. Furthermore, $0.8\,mg\,cm^{-2}$ Nafion® was applied onto the surface of each electrode. The Nafion® membrane 115, before being used, was first cleaned following a standard procedure, i.e.: (i) boiling membrane in 5 wt.% H_2O_2 solution of 80 °C for 1 h; (ii) rinsing with DI water of 80 °C for 1 h; (iii) boiling membrane in 0.5 M H_2SO_4 solution of 80 °C for 1 h; and (iv) rinsing with DI water of 80 °C for 1 h. Finally, the MEA was formed by hot pressing at 135 °C and 5 MPa for 3 min.

To avoid corrosion, the flow field plates, shown in Fig. 2, were made of 316 stainless steel [26–29] plates with a thickness of 2.0 mm. As can be seen in Fig. 2, the rectangular flow field plate consisted of two portions, the channel area and

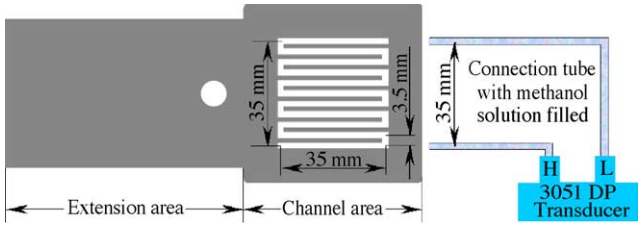

Fig. 2. Flow field plate and differential pressure transducer connection.

the extension area. The channel area acted as the distributor for supplying fuel and oxidant to the MEA, in which a single serpentine channel, $2.0 \times 2.0\,mm^2$, was machined by the wire-cut technology. The width of the ribs was 1.5 mm. The serpentine channel, having a total length of 420 mm, consisted of 11 long horizontal segments (35.0 mm in length) and 10 short vertical segments (3.5 mm in length). The extension area of the flow field plates served as a current collector. In addition, a tape heater was attached to the extension area to adjust the cell operating temperature to a desired value during the experiments.

The two enclosure plates, each having a thickness of 4.0 cm, were made of transparent Lucite material. Through the transparent enclosure plate, two-phase flow characteristics of gas CO_2 and methanol solution in the anode flow field could be distinctly visualized and recorded by the image recording system. It is worth pointing out that the Lucite material, having a low thermal conductivity, can effectively keep the heat, which generated in the MEA and provided by external heating, from dissipating to the surroundings under the conditions of higher operating temperatures.

2.2. Test loop

The experiments were carried out in the test loop shown in Fig. 3, which is detailed elsewhere [30,31]. Methanol solution was driven by a digital HPLC micro-pump (Series III). Before entering the cell, methanol solution was pre-heated to a desired temperature by a heater connected to a temperature controller. Simultaneously, high purity oxygen of 99.999% as oxidant was provided to the cathode side of the cell without humidification. The flow rate of oxygen was controlled and measured by a mass flow meter (Omega FMA-7105E) combined with a multiple channel indicator (Omega FMA-5876A). Similar to methanol solution, oxygen gas was also pre-heated to the desired temperature, and then flowed into the cathode side of the cell.

2.3. Measurement instrumentation and test conditions

In this work, a differential pressure transducer (Rosemont 3051CD series) was employed to measure the pressure drop between the inlet and outlet of the anode flow channel. Through two PFA tubes with an inner-diameter of 1/16 in., the high- and low-pressure sides of the transducer were connected, respectively, to the pressure taps located at the inlet and outlet of the anode flow field, as seen in Fig. 2. In this pressure drop measurement system, a fluid needs to be filled in the PFA tubes. To avoid any influence of the filling fluid on the cell performance, methanol solution was chosen as the filling fluid in the two PFA tubes, which had the same concentration as that fed to the anode flow field. The output by the transducer was transferred to a Personal Computer via a SI 35951 IMP board. A specially developed data acquisition program was used to monitor the pressure drop, and the data were stored in a computer hard disk for the post analysis.

An Arbin BT2000 electro-load interfaced to a computer was employed to control the cell operation condition and to measure voltage–current (polarization) curve. A pre-written schedule program was run to realize the control and measurement for a desired test condition. In this schedule program, the control mode such as current or voltage discharge, the accurate discharging value and duration, and data-sampling period were set in detail. All the tests in this work were conducted by selecting current discharge as control mode and scanning the current value from zero (i.e., open circuit) to a possible maximum value with an increment of 0.08 A (i.e., $5\,mA\,cm^{-2}$) for the range of smaller than $30\,mA\,cm^{-2}$ and

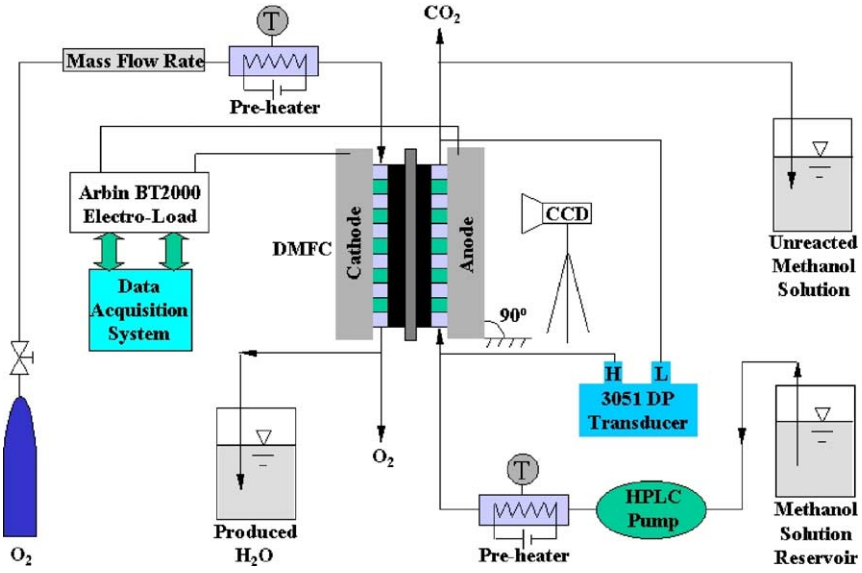

Fig. 3. Schematic of the DMFC test loop.

an increment of 0.16 A (i.e., 10 mA cm^{-2}) for the range of larger than 30 mA cm^{-2}.

Furthermore, a video and photo imaging system, including a JVC CCD, a NAVITAR 6X CCD C-Mount Len and a digital camcorder (SONY DCR-TRV900E), was employed to capture the images of the two-phase flow characteristics of gas CO_2 and methanol solution in the anode flow field. Being zoomed in by the NAVITAR 6X CCD C-Mount Len, the images of the anode flow field were shot by the JVC CCD and recoded on a Mini Digital Video Cassette by the digital camcorder.

All the experiments reported in this work were conducted for the fuel cell to be orientated vertically as shown in Fig. 3. The anode flow field was arranged as shown in Fig. 2, while the cathode flow field was fixed to be symmetric to the anode with respect to the MEA. Methanol solution entered into the anode flow field from the lower left corner, while oxygen gas was fed into the cathode flow field from the upper right corner. In such a flow configuration, it would be able to avoid the accumulation of produced gas CO_2 in the anode flow channel and of liquid water in the cathode flow channel. Furthermore, all the experiments were performed under the same cathode operation condition: a constant oxygen gas flow rate of 100 Standard Cubic Centimeter per Minute (SCCM) and atmospheric pressure (0.1 MPa).

2.4. Data reduction

For the present vertical fuel cell flow field, as seen in Fig. 2, the total pressure drop is obtained from

$$\Delta P_{TP} = \Delta P_m + \rho_c g \Delta h \quad (1)$$

where ΔP_m represents the measured pressure drop by the differential pressure transducer, while the term, $\rho_c g \Delta h$, denotes the hydraulic head caused by the altitude distance between the two pressure taps ($\Delta h = 35.0$ mm), with ρ_c representing the density of the filling liquid in the tubes connecting the pressure transducer to the pressure taps. The total pressure drop through the flow channel can be expressed as the sum of the frictional, acceleration, and gravitational terms:

$$\Delta P_{TP} = \Delta P_F + \Delta P_A + \Delta P_G \quad (2)$$

Under the open circuit condition, since no gas CO_2 is generated, the pure liquid (methanol solution) is in a forced motion by the pump. Under such a situation, the acceleration pressure drop becomes zero and hence Eq. (2) reduces to

$$\Delta P_{TP} = \Delta P_F + \Delta P_G \quad (3)$$

where ΔP_F is due to the single liquid flow only, and the gravitational pressure drop is given by

$$P_G = \rho_f g \Delta h \quad (4)$$

where ρ_f is the density of methanol solution in the flow field. Note that for the present vertically orientated serpentine flow field, the gravitational pressure drop is due only to the flow through the 10 vertical short segments, as the gravitational pressure drop through the 11 long horizontal segments is zero.

3. Results and discussion

3.1. General observation of pressure drop behavior

Fig. 4 shows the cell voltage polarization and the associated total pressure drop behavior through the anode flow field with current density under a typical cell operating condition with 2.0 M methanol solution fed at 1.0 ml min^{-1} and at 60 °C. Under the open circuit condition, corresponding to zero current density, the total pressure drop reads $\Delta P_{TP} = 35.36$ mmH_2O, which was, as indicated by Eq. (3), due to the gravitational pressure drop of 33.90 mmH_2O (calculated based on the density of 2.0 M methanol solution at 60 °C) and the frictional pressure drop of the single liquid flow of 1.46 mmH_2O (measured by the transducer). It is interesting to notice from Fig. 4 that during the cell discharging operation an increase in current density led to an increase in the total pressure drop. After reaching a peak at about 20 mA cm^{-2}, however, the total pressure began to decrease with current density. This behavior can be explained by analyzing the CO_2 gas bubble behavior in the anode flow field, as discussed next.

Fig. 5 shows the representative images of the CO_2 gas bubble behavior, corresponding, respectively, to Points A to D in Fig. 4. In these images, with the help of lighter liquid–gas interface, CO_2 gas bubbles can be distinguished from liquid methanol solution. The region enveloped by a lighter-grey liquid–gas interface represents a gas area, whereas the rest region in the flow field is the liquid area. As can be observed from the images for Points A and B corresponding to small current densities of 10 and 20 mA cm^{-2}, a rather small number of discrete gas CO_2 bubbles were generated and presented in the flow field, leading to an increase in both the frictional

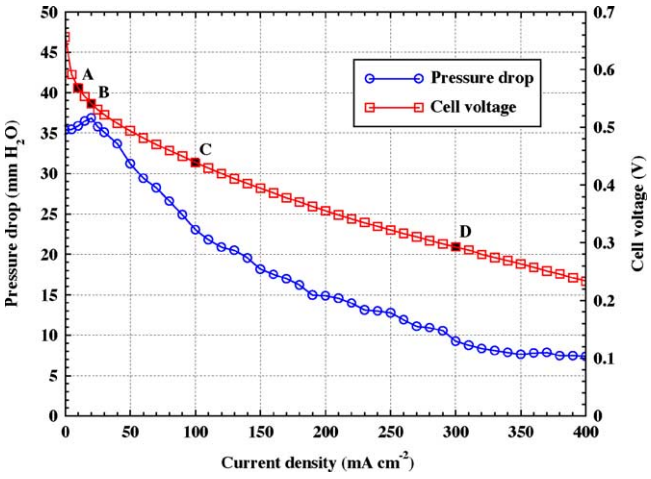

Fig. 4. Cell performance and the associated total pressure drop behavior with 2.0 M methanol solution fed at 1.0 ml min^{-1} and at 60 °C.

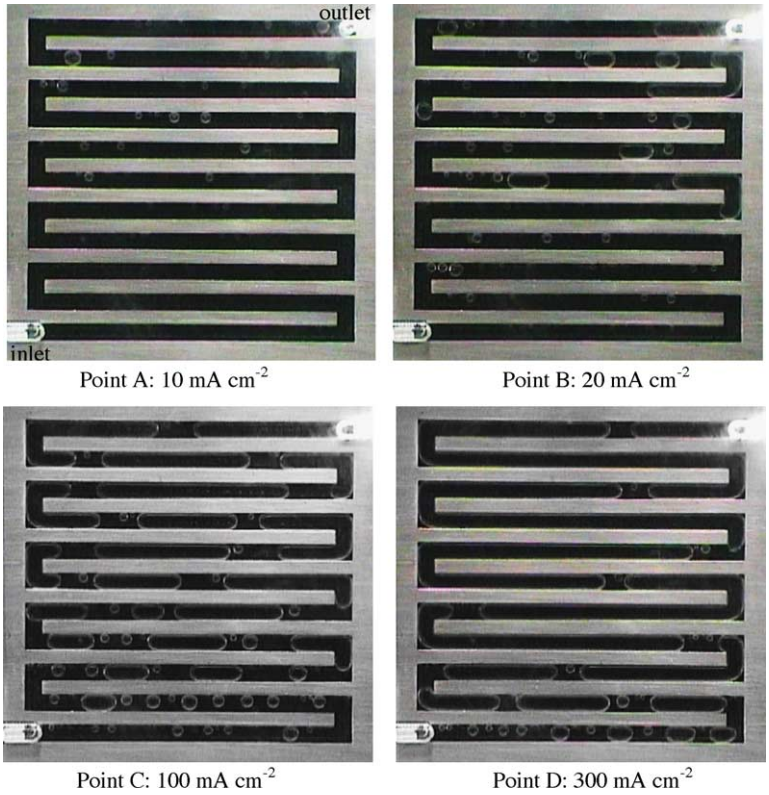

Fig. 5. CO_2 gas bubble behavior at different current densities with 2.0 M methanol solution fed at 1.0 ml min^{-1} and at 60 °C.

and acceleration pressure drops. In the meantime, these few gas bubbles had a little effect on the gravitational pressure drop because no bubbles were presented in the 10 short vertical segments of the serpentine flow channel and the average density was still the same as that of methanol solution. As indicated by Eq. (2), for the same gravitational pressure drop, the increase in both the frictional and acceleration pressure drops will cause an increase in the total pressure drop. This explains why the total pressure drops increased with increasing current density at low current densities shown in Fig. 4. However, as seen from the images for Points C and D, corresponding to high current densities of 100 and 300 mA cm^{-2}, many gas CO_2 bubbles were generated and presented in the entire anode flow field, including the horizontal segments and vertical segments. The increase in void fraction of gas phase leads to a smaller average density of two-phase fluid in the 10 vertical segments of the serpentine channel, which, in turn, results in a decrease in the gravitational pressure drop. Although the increase in void fraction of gas phase also causes a more or less increase in both the frictional and acceleration pressure drop, the decrease in the gravitational components becomes more pronounced, making the total pressure drop to decrease with increasing the current density as seen in Fig. 4. The experimental results presented in Fig. 4 indicates that for the vertically orientated DMFCs, high current density operation requires less pumping power for the fuel supply system, resulting in an increase in the overall DMFC system efficiency.

3.2. Effect of the methanol solution flow rate

Effect of the methanol solution flow rate on the total pressure drop behavior in the anode flow field at temperature of 60 °C is shown in Fig. 6. The experiments were conducted with 1.0 M methanol solution fed at flow rates of 0.5, 1.0, 2.0, 4.0, 8.0 and 10.0 ml min^{-1}, respectively. Under the open circuit condition, the total pressure drop was found to increase from 35.48 to 50.52 mmH_2O when the flow rate increased

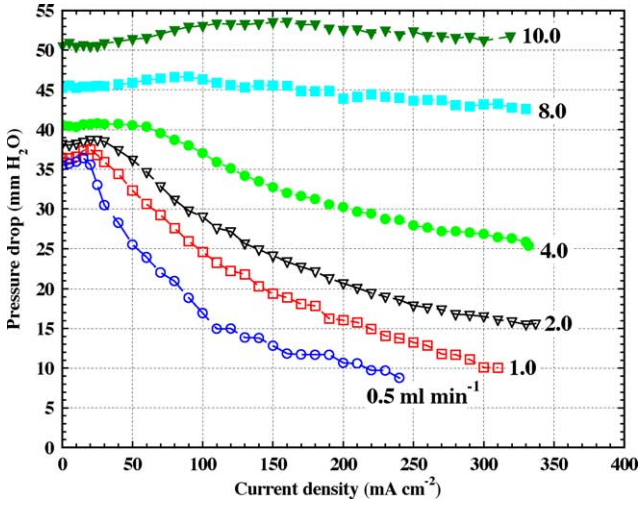

Fig. 6. Effect of methanol solution flow rate on the total pressure drop using 1.0 M methanol solution at 60 °C.

from 0.5 to 10.0 ml min^{-1} (see the vertical coordinate in Fig. 6). Furthermore, as seen in Fig. 6 that during the cell discharging operation, for a given current density, the total pressure drop increased with the flow rate. It is also interesting to note from Fig. 6 that when the flow rate was sufficiently high (e.g., 8.0 and 10.0 ml min^{-1}), the total pressure drop became almost independent of the current density. This phenomenon is attributed to the fact that higher flow rates caused the gas bubble removal rate from the flow field to become much higher than the bubble generation rate even at higher current densities. Under such a circumstance, a change in current density leads to a little change in void fraction of the gas phase and hence, the pressure drop becomes insensitive to the change in current density.

Fig. 7 shows the effect of methanol solution flow rate on the cell performance with the same operating parameters as in Fig. 6. As seen from Fig. 7, the cell performance kept improving as the flow rate increased from 0.5 to 2.0 ml min^{-1}, although this performance improvement was accompanied with an increase in the pressure drop as shown in Fig. 6. When the flow rate was higher than 2.0 ml min^{-1}, the cell performance became worse with increasing the flow rate. This is attributed to the fact that an increase in the methanol solution flow rate is accompanied by an increase in the static pressure in the flow field. A higher static pressure tends to increase in the methanol crossover from the anode to the cathode, leading to deterioration in the cell performance [30,31]. The experimental results shown in Figs. 6 and 7 imply that the operation of an entire DMFC system has to be optimized at an optimal flow rate, at which the highest cell performance is obtained with a less pumping power consumed for the fuel supply system.

3.3. Effect of cell operating temperature

Fig. 8 presents the effect of temperature on the total pressure drop behavior when 1.0 M methanol solution was fed at 2.0 ml min^{-1}. As can be seen from Fig. 8, for a given current density, increasing temperature from 23 °C to 60 °C resulted in a small decrease in the total pressure drop. There are two reasons associated with this phenomenon. First, the average viscosity and density of the liquid phase decrease with an increase in temperature, thereby resulting in a decrease in the frictional pressure drop. Secondly, lower CO_2 solubility in methanol solution and the evaporation of methanol solution at a higher temperature cause more gas phase present in the flow field, leading to a decrease in the gravitational pressure drop. Consequently, the total pressure drop decreased with increasing temperature. Fig. 9 shows the effect of temperature on the cell performance with the operation parameter being kept the same as the case shown in Fig. 8. Clearly, the cell performance, including OCV, potential and power density increased with increasing temperature from 23 °C to 60 °C. The maximum power density was about 70 mW cm^{-2} at 60 °C. The experimental results presented in Figs. 8 and 9

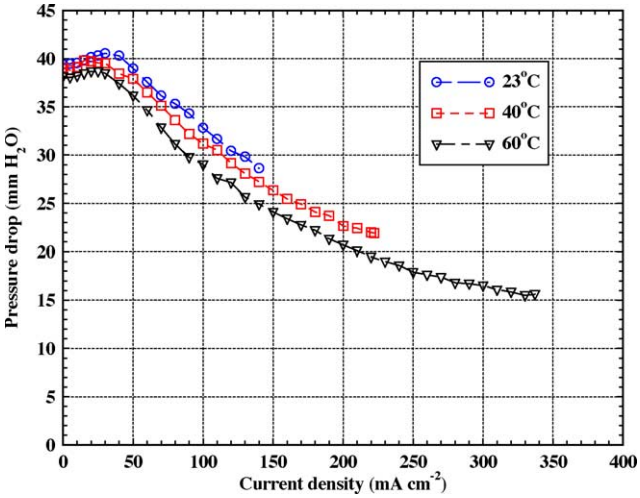

Fig. 8. Effect of temperature on the total pressure drop with 1.0 M methanol solution fed at 2.0 ml min^{-1}.

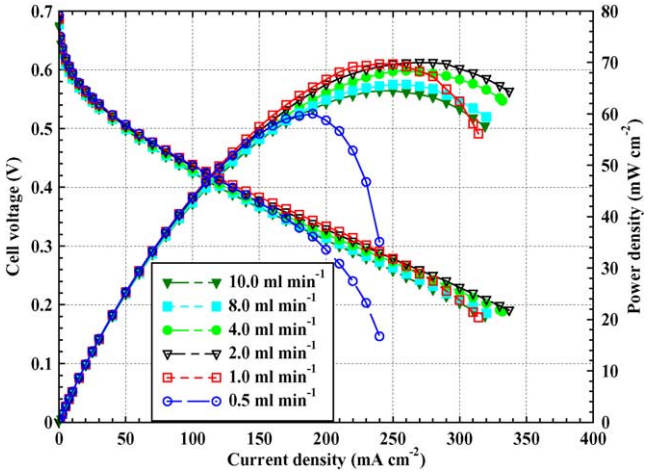

Fig. 7. Effect of methanol solution flow rate on the cell performance using 1.0 M methanol solution at 60 °C.

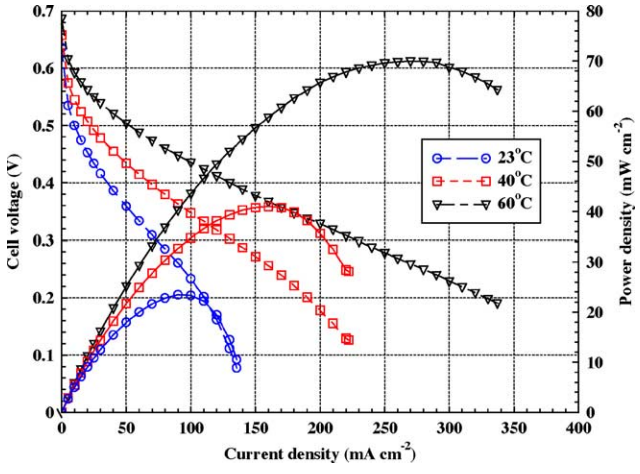

Fig. 9. Effect of temperature on the cell performance with 1.0 M methanol solution fed at 2.0 ml min^{-1}.

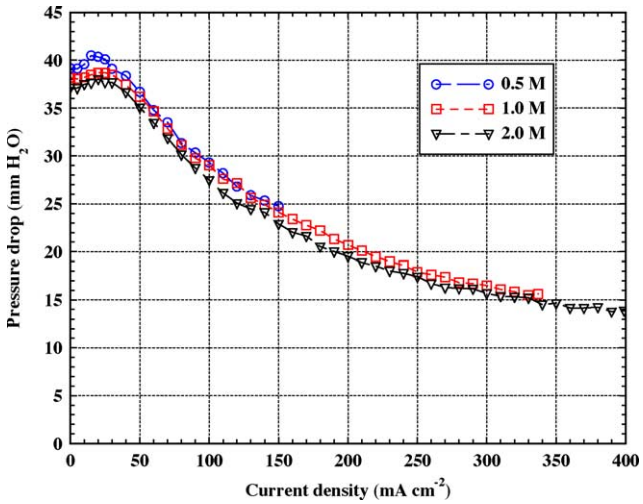

Fig. 10. Effect of methanol concentration on the total pressure drop at 2.0 ml min^{-1} and 60 °C.

reveal that an increase in the cell operating temperature leads to not only a significant improvement in performance but also a decrease, although rather small, in the pumping power for the fuel supply system.

3.4. Effect of methanol concentration

Effect of methanol concentration of 0.5, 1.0, and 2.0 M on the total pressure drop is shown in Fig. 10. This experiment was carried out with a fixed methanol solution flow rate of 2.0 ml min^{-1} and at 60 °C. As seen in Fig. 10, for a given current density, there was a rather small decrease in the total pressure drop when the concentration was increased from 0.5 to 2.0 M. In comparison with the temperature influence shown in Fig. 8, the effect of methanol concentration on the pressure drop was much smaller. This is attributed to the fact that the physical properties of methanol solution do not change that much when concentration increased from 0.5 to 2.0 M. However, concentration has an important influence on the cell performance. Fig. 11 shows the effect of methanol concentration on the cell performance with the same operating parameters as in Fig. 10. It is evident from Fig. 11 that the cell performance was improved significantly with increasing concentration from 0.5 to 2.0 M. The maximum power density was over 90 mW cm^{-2} with 2.0 M methanol concentration.

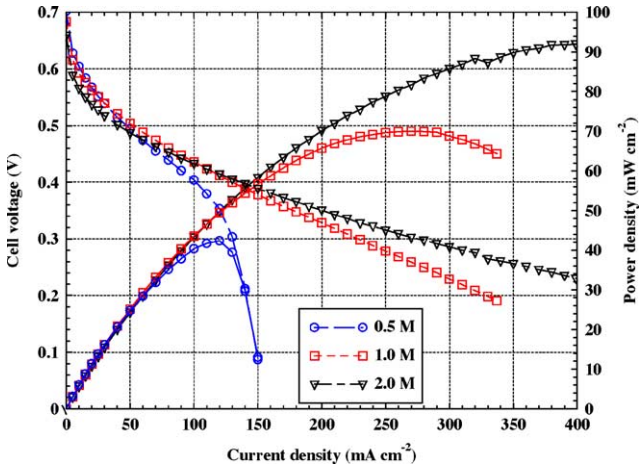

Fig. 11. Effect of methanol concentration on the cell performance at 2.0 ml min^{-1} and 60 °C.

4. Conclusions

The two-phase flow pressure drop behavior in the anode flow field of a vertical DMFC consisting of a single serpentine flow channel has been investigated experimentally. The experimental results show that at low current densities, the pressure drop increased with increasing current density. After reaching a peak at certain current density, however, the pressure drop began to decrease with increasing current density. It has also been shown that the pressure drop always increased with the methanol solution flow rate. However, either lower or higher flow rates deteriorated the cell performance. Therefore, in the practical operation of a DMFC system, special caution has to be taken to ensure an optimal flow rate to be selected, at which a better cell performance is obtained with a less pumping power consumed for the fuel supply system. The experimental results further reveal that the pressure drop became almost independent of the current density when the methanol solution flow rate was sufficiently high. The studies on the effects of cell operating temperature and methanol concentration reveal that both temperature and methanol concentration had a significant influence on the cell performance but they had a little effect on the pressure drop.

Acknowledgements

The work described in this paper was supported by a grant from the Research Grant Council (Project No. HKUST6197/03E) and a grant from the Innovation and Technology Commission (Project No. ITS/069/02) of Hong Kong SAR Government, China.

References

[1] M.A.J. Cropper, S. Geiger, D.M. Jollie, J. Power Sources 131 (2004) 57–61.
[2] R. Dillon, S. Srinivasan, A.S. Aricò, V. Antonucci, J. Power Sources 127 (2004) 112–126.
[3] V. Mehta, J.S. Cooper, J. Power Sources 114 (2003) 32–53.
[4] C.K. Dyer, J. Power Sources 106 (2002) 31–34.
[5] T. Schultz, S. Zhou, K. Sundmacher, Chem. Eng. Technol. 24 (2001) 12.
[6] E.H. Yu, K. Scott, Electrochem. Commun. 6 (2004) 361–365.
[7] X. Ren, M.S. Wilson, S. Gottesfeld, J. Electrochem. Soc. 143 (1996) L12.

[8] H.A. Gasteig er, N. Markovie, P.N. Ross Jr., E.J. Cairns, J. Phys. Chem. 97 (1993) 12020.
[9] S. Wainwright, J.-T. Wang, D. Weng, R.F. Savinell, M. Litt, J. Electrochem. Soc. 142 (1995) L121.
[10] S.C. Thomas, X. Ren, S. Gottesfeld, P. Zelenay, Electrochim. Acta 47 (2002) 3741–3748.
[11] S.C. Roy, P.A. Christensen, A. Hamnett, K.M. Thomas, V. Trapp, J. Electrochem. Soc. 143 (1996) 3073.
[12] M. Neergat, A.K. Shukla, K.S. Gandhi, J. Appl. Electrochem. 31 (2001) 373.
[13] B. Yang, A. Manthiram, Electrochem. Commun. 6 (2004) 231–236.
[14] R. Jiang, D. Chu, J. Electrochem. Soc. 151 (2004) A69.
[15] Y.-M. Kim, K.-W. Park, J.-H. Choi, I.-S. Park, Y.-E. Sung, Electrochem. Commun. 5 (2003) 571–574.
[16] X. Ren, T.E. Springer, T.A. Zawodzinski, S. Gottesfeld, J. Electrochem. Soc. 147 (2000) 466.
[17] Z. Qi, A. Kaufman, J. Power Sources 110 (2002) 177–185.
[18] J.P. Meyers, J. Newman, J. Electrochem. Soc. 149 (2002) A718.
[19] B. Libby, W.H. Smyrl, E.L. Cussler, Electrochem. Solid-State Lett. 4 (2001) A197.
[20] N. Jia, M.C. Lefebvre, J. Halfyrd, Z. Qi, P.G. Pickup, Electrochem. Solid-State Lett. 3 (2000) 529.
[21] J.G. Collier, J.R. Thome, Convective Boiling and Condensation, 3rd ed., Clarendon Press, Oxford, 1994, pp. 34–70.
[22] V.P. Carey, Liquid–Vapor Phase-change Phenomena: An Introduction to the Thermophysics of Vaporization and Condensation Processes in Heat Transfer Equipment, Hemisphere Pub. Corp., Washington, DC, 1992, pp. 411–435.
[23] H. Yang, T.S. Zhao, Q. Ye, Electrochem. Commun. 6 (2004) 1098–1103.
[24] P. Argyropoulos, K. Scott, W.M. Taama, Chem. Eng. J. 73 (1999) 217–227.
[25] P. Argyropoulos, K. Scott, W.M. Taama, Chem. Eng. J. 73 (1999) 229–245.
[26] J. Ihonen, F. Jaouen, G. Lindbergh, G. Sundholm, Electrochim. Acta 46 (2001) 2899–2911.
[27] D.P. Davies, P.L. Adcock, M. Turpin, S.J. Rowen, J. Power Sources 86 (2000) 237–242.
[28] D.P. Davies, P.L. Adcock, M. Turpin, S.J. Rowen, J. Appl. Electrochem. 30 (2000) 101–105.
[29] E. Middelman, W. Kout, B. Vogelaar, J. Power sources 118 (2003) 44–46.
[30] H. Yang, T.S. Zhao, Q. Ye, A study of CO_2 gas bubble behavior in a direct methanol fuel cell, in: Proceedings of the Second International Conference on Fuel Cell Science, Engineering and Technology, Rochester, New York, USA, June 14–17, 2004.
[31] H. Yang, T.S. Zhao, Q. Ye, J. Power Sources 139 (2005) 79–90.